

Poly-Saora Robotic Jellyfish: Swimming Underwater By Twisted and Coiled Polymer Actuators

Armita Hamidi¹, Yara Almubarak¹, Yash Mahendra Rupawat¹, Jeremy Warren¹, and Yonas Tadesse¹

¹Humanoid, Biorobotics and Smart Systems (HBS) Laboratory, Mechanical Engineering Department, Jonsson School, The University of Texas at Dallas, Richardson, TX, USA.

Abstract

Jellyfish are energy-efficient swimmers due to the muscle-powered flapping of their soft bell that facilitates a unique energy recapture mechanism. In this paper, we present a bio-inspired jellyfish robot named Poly-Saora that mimics the swimming behavior of the jellyfish species *Black sea nettle (Chrysaora achlyos)*. An assembly-based fabrication method is used to create the Poly-Saora that is developed mainly with polymeric materials (95% of the robot by volume). Twisted and coiled polymer (TCP) actuators are successfully implemented in this robot and show great potential for underwater applications. The influence of different parameters such as the amplitude of the input power, the actuation frequency, and the lifecycle of the actuator are investigated underwater. A full characterization of 6-ply TCP muscles is demonstrated. An actuation strain of $\sim 10\%$ is achieved in water at a frequency of 0.1Hz and 50 kPa load. When integrated into the jellyfish, the TCP was able to bend a single bell by 17° . Poly-Saora was able to swim a vertical distance of 180 mm in 220 s with four TCP actuators each confined in a separate conduit. The robot mimics the swimming behavior of a real jellyfish by contracting the bell segments through the activation of the actuators, which generates forced water circulation under the bell in a pulsating rhythm, consequently creating a vertical movement of the robot. Overall, Poly-Saora is presenting a model of an underwater system that is driven by stimuli-responsive polymer materials and has unique advantages over conventional rigid robots due to their lightweight, muscle-like structures, silent actuation and ease of manufacturing. This robot can be used for safe interaction with other underwater species and their natural habitats when fully developed.

Keywords: Underwater robots, biomimetic robot, jellyfish, TCP actuators, soft bell deflection.

1. Introduction

Since their inception, several robotic and biomimetic machines have focused on motors and pneumatic or hydraulic pistons to produce mechanical motion. Conventional robots have many motors and complex control systems that work together to maximize efficiency and provide movement. Although this has become a standard in most current robots, these ‘hard’ actuators can also lead to issues such as safety, overheating, cost, and can become extensively complex. Due to recent rapid technological developments, robots are required to perform important tasks in applications such as medicine, search and rescue, disaster response, and human assistance [1]. Therefore, they should be able to handle unexpected interactions with unstructured environments such as functioning underwater. Developing small underwater biomimetic robots is still difficult due to many factors such as selecting actuators that must be safe and efficient for underwater propulsion, sealing the electronics, compactness, wireless motion control, reducing noise, and high propulsive efficiency even at micro level [2].

Smart materials are the basis of many applications such as sensors and actuators. Most smart actuators have the potential to demonstrate similar physical properties (stiffness, elasticity, strength, and density) as biological tissue. It is important to recognize that almost all biological organisms, and certainly all animals, rely on softness. They exploit their softness to bend, twist, and squeeze in order to change shape, hide, and move.

Previously, smart actuators used in underwater robots include, shape memory alloys (SMA) [3-6], dielectric elastomer actuators (DEA) [7, 8] and ionic polymer-metal composite (IPMC) actuators [9-14]. A summary table is provided in table 1 that consists of information such as size of the robot, type of actuators used, and the speed. These actuators are primarily used to either create oscillation or jet propulsion induced motion to allow the robot to swim underwater. Oscillatory motion of biomimetic fins imparts greater forward thrust and swifter turning capabilities. This was demonstrated by the successful testing of an acoustically controlled soft robotic fish in the Pacific Ocean by a group of researchers at MIT [15]. In the past decade, several bio-inspired fish [2,13,14] and manta ray (*Mobula birostris*) [4,7,11,12] have been developed using smart actuators that are propelled by the oscillatory motion of biomimetic fins. Many biomimetic jellyfish have been developed and studied over the years by working on the principle of jet propulsion induced motion as well as rowing motion. Their practical application was successfully demonstrated in the Atlantic Ocean by a group of researchers at the Florida Atlantic University using an untethered, hydraulically actuated, soft-robotic jellyfish that could also navigate through orifices [16]. A pneumatic based actuation, Fludojelly (220 mm in diameter) was recently demonstrated in Joshi et al. [17], which was able to carry a 100 g load and swim vertically at a speed of 160 mm/s. Smart actuators find an important application in the development of soft-robotic jellyfish due to their highly compliant configurations and adaptability in unstructured environments. Najem et al. [18] presented the development of robotic jellyfish using IPMC actuators that reached a maximum speed of 1.5 mm/s. In another study, Villanueva et al. [5] developed a jellyfish robot called Robojelly using SMA actuator to achieve a proficiency of 0.19 s^{-1} , which is comparable to its biological counterpart that has a proficiency of 0.25 s^{-1} .

Twisted and coiled polymer (TCP) muscles are inexpensive and high strength actuators that can appropriately match the performance of mammalian skeletal muscles [19]. **Here, in this work, we hypothesize that extremely twisted and coiled silver-coated 6-ply TCP actuators can results a good swimming characteristics of a robotic jellyfish, when used in a suitable structures and optimum actuation conditions.** Using these actuators in robots help maintain a relatively small weight and volume compared to those fabricated using conventional motors and pneumatic actuators. Employing lightweight artificial actuators that create more space for on-board sensors and exploration devices, will have a meaningful impact in the field of underwater discovery, pollution detection, and video mapping [10].

In this study, we showed the potential of using twisted and coiled polymer (TCP) actuators in an underwater biomimetic robot. Inspired by a real jellyfish, we exploited the swimming capability of our robot by utilizing a 3D printed polymer structure and polymer actuators (**Fig.1**). Jellyfish are underwater sea creatures with soft bodies and anatomies. They are the earliest animals known to swim via jet propulsion produced by contracting circular muscle fibers in their bell [20]. They have high swimming efficiency, which is an attractive design alternative for many engineering applications that require improved efficiency for underwater applications. The body of the jellyfish consists of a dome-like bell and long hanging tentacles. Our jellyfish robot consists of three major parts, namely, the silicone bell that resembles the jellyfish umbrella, a 3D printed structure that contains 8 channels for placing the TCP actuators peripherally around the bell, and the TCP muscles themselves as the actuators. This initial design of the robot is inspired by Tadesse et al. [21], which is modified to use TCP actuators/muscles in this work. The robot has a polymeric structure that houses the polymer muscles that induce motion. This fact helps us to develop the structure for underwater application without requiring any sealing procedure due to the compatibility and

good actuation behavior of the polymer muscle in water. Unlike many structural alloys and pure metals, which can be strongly affected and corroded due to exposure to moisture, polymers are more resistant to chemical reactions and have long-lasting performance in water. However, the sealing structure can reduce the power consumption of the robot and consequently, increase its efficiency. The sealing will also help the safe operation of the robot in water as currently high current is provided to the actuators. Moreover, the low-profile actuators make the robot compact and lightweight. The total weight of our robot with all components is 440 g. One of our research goals was to investigate the actuation behavior of the bell under different geometrical and input conditions. Our challenge was to employ key features to enable this novel biomimetic prototype to swim using advanced materials and actuators. By focusing on the deformation of the bell segment, accumulating vital performance data such as mechanical stress and elastic deformation, pre-stress, loading condition, and improving its operating conditions, Poly-Saora was capable of swimming underwater. During swimming, the TCP muscles provided the bell contraction and relaxation motion, and the jellyfish structure moved due to this deformation. This design can bring a new paradigm of research in the realization of all-polymer based underwater robots that is not demonstrated so far. **Poly-Saora is the first robot to demonstrate the practical application of the silver-coated nylon 6,6 TCP_{Ag} muscle in water, highlighting many advantages of these inexpensive, compact, and light-weight polymer actuators. This robot is customizable and one can change the actuators easily (4, 6, 8 - ply) based on the requirement and application.** In summary, the significant results of this paper are the following:

- A biomimetic jellyfish robot is designed and developed to closely mimic the real jellyfish. Both the structure and the actuators of Poly-Saora are fabricated entirely by polymer materials which include 95% of the total volume of the robot. The utilization of mainly polymers (silver-coated nylon 6,6, TCP_{Ag}) to create a noiseless actuation method and lightweight structures makes Poly-Saora unique and unlike any other conceived.
- We have used the twisted and coiled polymer (TCP) actuators in an underwater structure for the first time. Due to the thin polymer muscles (less than 2.5 mm diameter), this robot has great potential for the development of compact design and underwater discovery applications without any harmful effect on the underwater ecosystem.
- A successful underwater swimming test was performed using TCPs for the first time. The robot was able to swim vertically a total distance of 180 mm in 220 s by actuating four bells. The conical shape robot has a size of ~210 mm in diameter and 200 mm in height, and its weight is 440g.
- A full muscle characterization in underwater condition is performed, which is not available in the literature so far. The results reveal the effect of active cooling of the muscle submerged in water and determined the best actuation parameters for TCP. The 95-mm long muscle can reach ~10 % actuation strain by passing 0.09 W/m electrical power for 1s underwater. The conducted results are useful data for any other application of TCP in water. Moreover, brief pauses during actuation to cool the TCP actuators were used as an advantage to allow the flow circulation developed under the bell structure in each swimming cycle.
- The bell actuation mechanism is studied based on the material properties and the geometry of it. Analytical and experimental relations between the load and the deflection angle of the jellyfish bell are presented. It is shown that a single bell can rotate 17° by the TCP actuator confined in a conduit. The life cycle of 6-ply TCP used for the robot indicated sustaining ~800 cycles when a power which 3 times higher than the standard power (electrical current of 7A) is applied in cyclic loading in water at 0.25 Hz frequency.

The rest of the paper is organized as following: in section 2, we discuss the fabrication of the Poly-Saora structure and the TCP actuators; in section 3, the results of the swimming mechanism, a comparison to the real jellyfish, is discussed and comprehensive muscle characterization in underwater condition is also

presented. Moreover, the bell deflection angle is studied considering the effect of the silicone bell thickness followed by the varying of the TCP's initial pre-tension for actuation. The final part, section 4, includes the conclusion and future work.

2. Design and Fabrication

2.1. Bioinspired jellyfish robot design and working principles

The swimming mechanics of the real jellyfish is simple but functional. During swimming, the muscles activate alternating cycles of contraction followed by the relaxation of the bell driven by elastic recoil [22]. **Black sea nettle (Scientific Name: *Chrysaora achlyos*) shown in Fig. 1(a) & (b) is a giant jellyfish and the largest invertebrate discovered in the twentieth century. This species was not classified until 1997 and was not studied that much compared with others such as moon jellyfish [23]. It has unique overall structures, bell geometry and oral arms that attracted our attention. It has large anchoring structures that allow it to swim headfirst into strong oceanic currents. Its size can reach up to 3 feet (1 m) and its oral arms extending to 20 feet (6 m)[24]. The unique oral arms that extend from the bell closely match to the bioinspired robot we conceived, a robot having actuators configured around the bell in distinct hollow channels. We were inspired by this unique structure, and tried to make the smaller size, and study the behavior.** In this study, we attempted to follow the same fundamentals in the jellyfish structure to prepare it for maneuvering underwater as shown in **Fig. 1(c)**. The bioinspired robotic jellyfish prototype is designed and fabricated in a way to mimic the flexible motion characteristics of the jellyfish bell during swimming. As shown in **Fig. 1(d)**, the structure consists of a bottom case, a body, and a cap that are 3D printed using ABS polymer. The soft bell is cast by using an equal amount of 150 mL of part A and 150mL of part B of Ecoflex 00-30 (Smooth-On, Inc.) in a circular plate with a diameter of 210 mm and thickness of 3 mm. Two holes are placed in the center of the circle to accommodate the designed cap inlets. Ecoflex is a light density (1040kg/m^3), room temperature vulcanized (RTV) silicone, which is suitable for a variety of applications including making prosthetic, orthotic devices and soft robots. Eight spring steels with 0.1 mm thickness are mounted under the bell and attached to the body from one end. These spring steels behave as passive membranes to help the bell relax back to its original position after actuation and replicates the passive energy recapture phase of the real jellyfish swimming following the bell relaxation [22]. The hard body of the robot has eight channels to be able to insert eight muscles, each 95 mm in length. The muscles are fixed to the bottom of the body using small plastic end stoppers. A smaller case consisting of eight pulleys is used for transmitting the TCP muscle power to the bell segment (**Fig.1(e)**). During the muscle actuation, the TCP contracts and pulls the bead wire, which is passed through the guides attached to the spring steel and then fixed at the tip of the spring. This results in bending the spring steel and consequently a contraction in the bell as shown in **Fig. 1(f)**. The muscles are powered and controlled through copper wires that are connected to a DC power supply placed out of the water. All the wires pass through the top cap inlet and therefore, will not interfere with the robot's motion. All the fabrication steps are summarized in **Fig. 1(g)**.

2.2. Actuator fabrication

The twisted and coiled polymer (TCP) muscles were fabricated by a semi-automated apparatus by suspending a dead weight at the bottom end of a polymer thread while connecting the top end to a motor as shown in Supplementary Fig. S1. A video of the fabrication process for 2-ply TCPs can be found from HBS Lab Youtube Channel https://youtu.be/S4-3_DnKE9E . We followed a similar procedure and setup but produced different structures such as 4-ply and 6-Ply TCP. The number of required threads depends on the type of muscle desired. N threads (extremely twisted & coiled) are used for a 2N-ply muscle. A dead weight of $N \times 175$ grams (for example 175g for 2ply TCP [25]) is used for the process. The twist was achieved by applying a counter-clockwise rotation using the motor. This twisting process is allowed to occur until the entire length of the thread is coiled, which results in N-ply coiled polymer. In order to make 2N-ply muscle,

we folded the N-ply in half and due to the initial rotational tension, the second coiling process is done manually [26]. Then the muscles were crimped on both ends using brass crimps. The muscles were then annealed by suspending the dead weight and applying a sequence of input current ($N \cdot 0.75A$, i.e. $1.5A$ for 4ply TCP) at various heating and cooling cycles until the actuation strain reaches steady state. For, this robot, we have fabricated a 6-ply silver-coated TCP actuator using 3 threads of equal length that are tied together at both ends and then coiled. The fabricated 6-ply actuator is then trained and annealed at an input current of $2.2A$ producing an average actuation strain of 19 %. The cost of 95mm 6-Ply TCP is around \$0.4 or \$2600 per kilogram of the same actuator. This is equivalent to \$4.5/m for 6-ply TCP. In general, TCPs are low cost actuators and have several advantages [27, 28]. Twisted and coiled polymer actuators/muscles made out of silver-coated nylon 6,6 (TCP_{Ag}) are relatively expensive than the TCP made out of monofilament nylon fishing line (TCP_{FL}) that are utilized for actuating robotic a finger [29]. They cost \$5 per kg as the heating source is cold and hot water, they don't need heating elements such as nichrome [30].

3. Experiments and Results

3.1. Swimming test

The most important parameters to make the robot swim like a real jellyfish are the contraction frequency, the bell profile during contraction and expansion, mass and buoyancy, large rotations of the bell through a fluidic medium, and interaction between the structure and the surrounding fluid. The flapping frequency of the bell is the first important parameter directly related to the muscle actuation frequency. When the TCP actuators are immersed in water, they can be electrothermally actuated at 5Hz to produce ~10% strokes [19]. However, the best actuation frequency is the one that provides enough bell deformation for rowing motion. Flapping the bell at 0.25 Hz (1s heating followed by 3s cooling) provided enough bell deformation to move the jellyfish underwater. Similar to the real jellyfish presented in [22], brief pauses during actuation to cool the TCP actuators can be an advantage to allow for the full development of the flow circulation for a single swimming cycle. Moreover, having such a lightweight actuator (0.841 g for one 6-ply TCP) keeps the total weight of the robot at 440 g and allows it to easily achieve neutral buoyancy under the water by adding a small piece of foam to the structure.

Efficient propulsion is another important factor that was considered for successful swimming. When the bell pushes against the fluid, a pressure gradient is generated across the bell surface that leads to the forward acceleration of the robot. The structure would move forward at each actuation pulse, but during the relaxation of the bell (cooling the muscle), it would sink slightly due to its own weight. This swimming pattern of the jellyfish robot is shown in **Fig. 2(a)**, when the robot swims a total vertical distance of 180 mm in a fish tank **by actuating the muscles in 55 cycles**. Only four bells are used for swimming and each muscle (length $L = 95\text{mm}$ and the resistance for each actuator is $R = 2.5\Omega$) is actuated at an input current of 7 A for 1s heating with 3 s cooling (0 A). Increasing the input current is essential for muscle actuation when the TCP is submerged in water due to the rapid cooling process provided by the fluid. We will seal the entire system in the future for the safe operation of the robot in water, as currently high current is provided to the actuators. The maximum vertical speed of the prototype at each pulse is 5 mm/s. The proficiency (velocity normalized by the bell diameter) of our prototype is 0.024 s^{-1} . **The maximum velocity is higher when the jellyfish is at the bottom of the tank, and it reduces when the robot gets closer to the surface, due to the change in pressure and heat accumulation in the channels. Since the circulation is less, the TCP actuators are not cooled down at the end of each cycle and therefore, there will be a decrease in the actuation strain, which consequently reduces the speed of the swimming. Future works include integrating sensors and measuring the temperature at different height of the water column.** Moreover, the velocity pattern (rising and falling) is very similar to the speed variation in the real jellyfish during bell contraction and relaxation cycles as illustrated in [22]. The undulatory motion of the bell margin is also

observed during the swimming as shown in **Fig. 2(b)**. During the contraction phase of the swimming cycle, the inward bending at the bell margin occurred, which converted to an outward bending at the tip of the bell at the end of the relaxation phase. This result is also comparable to the *Aurelia aurita* jellyfish species which has similar changes to the bell margin to control and enhance the vortex rings around its body during swimming [31, 32] and shown in **Fig. 2(c)**. All video recordings of Poly-Saora robotic jellyfish were conducted in a 70-gallon fish tank ($92 \times 58.5 \times 46 \text{ cm}^3$) in a lab setting containing tap water at 20° C . **The swimming video is also provided as supplementary <https://youtu.be/sDEk2Y38Bzg>.**

The input power for heating the actuator is another important variable to provide efficient bell deformation for swimming. To study different actuation characteristics, the bell actuation angle is compared using 4-ply and 6-ply TCP muscles at different input powers (heating energy). Three different bell geometries are studied here. As shown in **Fig. 2(d)** the 6-ply muscle provided a maximum deflection of 13° at 9.5A, which is twice the bending provided by 4-ply muscle at 7A. It is important to note that each muscle can withstand a maximum current input depending on its resistance before breaking; this will be discussed further in the TCP characterization section. Due to the surface area of the silicone flap and its connection to the center, the flap experiences a small resistance to bending. As the slits extend toward the center and the bell section separates farther from the center (longer slits), it can move more freely and bend more effectively. As shown in **Fig. 2(d)**, the bell with longer slits (P1) bent up to 16° when an input current of 8.8A supplied to the 4-ply TCP actuator. However, this long slit bell configuration is not capable of swimming because if the bell components are separated, it will allow the water to slip between them (on the sides) and the pressure gradient reduces under the bell.

The total electrical power applied to Poly-Saora for swimming was 600 W. In general, the TCPs consume lower power while actuating in the air. The high energy consumption is attributed to the fact that the TCP muscles are used underwater. In general, the TCP has much lower power consumption while actuating in the air. When the TCP submerged in water, the increase in input power is necessary to reach the actuation temperature needed to move the muscle due to the rapid cooling of the muscle. Moving forward, isolating the muscles from the water will decrease power consumption. This can be done by circulating water, which is isolated for the surrounding. More work should be done on the material side to reduce power consumption.

This is the first iteration of the robot. The goal here is to test this new actuation technology for the robot and determine the behavior, and possibly optimize the robot in future. The current actuation frequency of the robot is 0.25 Hz, which is lower than the real jellyfish (1.1 Hz) [33]. However, it is still a higher TCP actuation frequency compared to other works that use the same actuators in dry state. We have not used an active cooling in the channels and those are left for future works. TCP actuators can operate at higher frequency 5-7 Hz [19]. However, we are not concerned about the speed at this time considering the number of variables that we need to study. The issue of frequency is important in some applications and needs further study.

3.2. TCP_{Ag} characterization by actuating underwater

In this section, we present the results of several experiments that were performed on the 6-ply TCP actuator in water. The length of the muscle is 95 mm (the same length used in the robot for swimming), the resistance R is 2.5Ω , and the diameter D is 2.4 mm. The aim of this test is to study the parameters of the actuators under different conditions. **Fig. 3(a)** shows a snapshot of the different structures of the actuators that can be fabricated using the method explained earlier. **Fig. 3(b)** shows a schematic diagram of the experimental set up for testing. A cylinder filled with 5.5 gallons of water is used to submerge the muscle. Calibrated weights are attached to the bottom of the actuator in the water and the top end is fixed. Copper wires are

connected to both crimps on the ends of the actuator and to the DC power supply, which is located next to the setup. A thermocouple is connected around the midpoint of the actuator to measure the temperature profile during the heating and cooling cycles. NI 9219 is used to measure the output voltage, the NI 9219 is used to measure the temperature, and an open source tracking program (tracker physics) is used to capture the displacement from a video recording. All the data were saved and plotted using MATLAB. The 6-ply TCP muscle is tested by hanging a 50 kPa load (900 g mass) on one end and fixing the other end while it is fully submerged in water. Typically, when the TCPs are used in air, they are actuated at low frequencies due to the time requires for cooling. However, the actuation frequency can be increased to 10Hz when the muscle is directly actuated underwater due to cooling effect. The properties of the TCP muscle actuated in the air and in the water are compared in **table 2**. The maximum displacement and temperature of the muscle are measured at two different frequencies underwater as shown in **Fig. 3**. The muscle was actuated with a power input at almost 3 times more than the standard power consumed in an open-air environment. The maximum actuation strain produced at 0.1Hz and 0.25Hz frequencies is 8% and 5%, respectively as shown in the 1st row of **Fig. 3(c and d)**. There is a bias for both frequencies due to insufficient cooling (9s at 0.1Hz and 3s at 0.25Hz). The temperature of the muscle remained under 60°C as shown in the 2nd row of **Fig. 3(c and d)** while actuating in water and therefore, the actuation strain is less than when the actuation is in air. It is reported that the temperature of the actuator would reach 140°C when it is actuated in air [34]. This result can be compared to Wu et al. [35] who reported 14% stroke for a 2-ply muscle in the air with an input power of 2.15 W/cm heating for 1s. It is observed that if the frequency increases to values higher than 1Hz, there is a sudden drop in the displacement with a high bias that will affect the efficiency of the muscle. The sampling rate for temperature, voltage and current data shown in **Fig. 3(c and d)** was 10 Hz while the displacement was analyzed by Tracker (open source video analysis) software and the samples were read at 2.5 Hz.

In order to show the consistency of the muscle, a lifecycle test was conducted for the 6-ply TCP actuator with the same length (95 mm) directly exposed to the water. The jellyfish structure is fixed inside the water tank. Test results such as the time domain plots of the actuation strain, temperature change, input current and output voltage of the 6-ply TCP muscle are shown in **Fig. 4**. The 6-ply TCP continuously operated for a total of 787 cycles. This result shows the uniform behavior of the muscle in a number of cycles as shown in the amplitude of the actuation strain plot at the bottom left of **Fig. 4**. Here, the actuation strain amplitude maintained at an average of 10%. These results are very dense due to the long test time, thus we showed actuation strain, actuation temperature, input current, and output voltage zoomed sections between 346th and 356th cycles (an equivalent time of 40 s) in the inset of each figure. It is important to note that this power consumption of the muscle is still 3 times higher than the one used in standard air actuation. A bias can be observed, which increases as the number of cycles increases due to the heat accumulation of the surrounding water. **As it is shown in Fig. 4, the voltage is increased as the number of cycles increased and therefore, the resistance of the muscle increased ($V=RI$). This is due to the reaction between the silver particles and the water. By passing the electrical current through the silver coated nylon 6,6, the silver particles react to the water and oxidize. It is also observed that after prolonged actuation of the muscle in water results in change in color of the muscle to dark brown due to this reaction in water. The training of the muscle is done in the air and then the actuation was done in a different environment (water). The obtained results suggest that a different training procedure for annealing the muscle in water, which needs further investigation in the future.** Saharan et al. [36] reported a lifecycle of 200 at an input voltage of 11V for 25s (0.04 Hz) with a 20% duty cycle for 2-ply TCP. A comparison of the characteristics of TCP muscle in air and water shows that the strain actuation decreased in the water while the lifespan of the muscle increased significantly, and the muscle can actuate at much higher frequencies (up to 10 Hz) due to active

cooling. Coiled nylon wrapped with multiwall nanotube (MWNT) can sustain a million cycles before failure [19], however adding MWNT will add cost. Therefore, we studied the TCPs (6-ply) for the lifecycle.

3.3. Soft Bell characterization

Ecoflex 00-30 is used to prepare the soft segment of the jellyfish in this study. For this study, instead of using the TCP actuator to bend the bell, calibrated weights are used ranging from 10 to 700g. The muscle is removed from one channel and instead, the spring steel is loaded through the pulley system by calibrated weights to measure the deflection angle on each load as shown in **Fig. 5(a)**. The flat spring steel plates are used to further control the stiffness of the bell and maintain the structural rigidity. Each bell segment is embedded with one spring steel. The thickness of the spring steel used for Poly-Saora robotic jellyfish is 0.1mm, which provides enough stiffness for the bell to deform by actuating the TCP and returning it back to its original position when the muscle stops actuating. **The relation between the required force and the deflection angle of the spring steel is shown in Fig. 5(b)**. By decreasing the thickness of the bell, a lower force is required to bend the bell. **Fig. 5(c)** shows the displacement of the bell with 3mm in thickness and 120 mm in length under different loads. Increasing the thickness and stiffness of the bell requires a more powerful actuator or an array of muscles for each bell, which in return will require greater energy to operate the robotic structure. Deflection analysis is done to gain an understanding of the force-deflection characterization of the bell. The bell bending is due to the deflection of the spring steel, which can be assumed as a cantilever beam effect with transverse load at the tip. However, adding the silicone bell will affect the stiffness. In this study, we assumed the spring steel as a rectangular cantilever beam under direct compression and bending forces. Due to the high ratio of the length to the thickness of the spring steel, the shear stresses can be neglected. The spring steel restore the deflection and recover to its straight shape, but the effect of the bending moment is the main reason for deflection. If the bending moment increases in the constant stiffness structure, the beam continues to bend until it fails.

The deflection of the beam can be derived from Euler cantilever beam using equation (1) [37]:

$$\theta = \frac{FL^2}{2EI} \quad (1)$$

Where θ is the deflection angle, F is the applied bending force (F_y , perpendicular to the spring steel axis) at the tip, L is the length of the spring steel, E is the elastic modulus ($E=200$ GPa for 1095 steel) and I is the moment of inertia, which is related to the geometry of the cross section. The analytical results of spring steel deflection obtained using Equation (1) are shown in **Fig. 5(c)**. These results were used to predict the angle between the applied force and the spring steel. In this regard, the same experiment mentioned previously (**Fig. 5(a)**) is conducted on the jellyfish structure without the silicone bell to find the relation between the force applied and the deflection angle produced. The experimental results were matched to the theoretical values conducted from Euler cantilever beam (eq.1) and the angle is calculated. This angle is small ($\beta=0.6^\circ$), and it showed a good agreement with the results predicted analytically as shown in **Fig. 5(c)**. The larger component of force, which is parallel to the spring steel axis results in compression loading. This effect can be calculated from equation (2) [38]:

$$\delta = \frac{FL}{AE} \quad (2)$$

Where δ is the deflection due to the compression, A is the area of the cross section, L and E are the same as Equation (1). The effects of compression (by axial force) are neglected in this study since the calculated

values are so small. For instance, the beam axial deformation on the maximum loading of 700g (~7N), when the spring steel is fully bent and is in contact with the 3D printed body, is only 0.006 mm.

The resistance of the beam to bending can be measured by flexural rigidity (EI) which depends on the material and geometry [39]. The flexural rigidity of the bell is calculated as 0.47 MPa.mm³. For the bell with higher thickness, flexural rigidity is higher and therefore, it requires larger forces to bend.

Based on the obtained results from the bell actuation using 6-ply TCPs and swimming tests (**Fig.2(d)**, green lines, 6-ply at 8.8A-0.2kJ energy) presented in the previous sections, the bell should be actuated to reach a minimum of 10 degrees bending angle to provide sufficient propulsion for the jellyfish robot to swim. As shown in **Fig. 5(b)**, the bell with 3 mm thickness required ~2N force to bend 10 degrees. This bending angle can be achieved by a 95 mm TCP muscle with 800 g pretension actuating at a strain of 7 %.

3.4. Effect of TCP pre-tension on the actuation of one bell segment

In this part of the study, we have determined the effect of muscle pre-tensioning to study the actuation strain while operating in the jellyfish structure. It is determined that suitable pre-tensioning is highly important to get the best actuation from the actuator. This is mainly due to the spacing between the coils of the actuator. However, very high pre-tensioning results in the breaking of the muscle during the first actuation cycle. In order to vary the pre-tensioning of the muscle, a longer TCP actuator with a length of 310 mm is chosen to extend the muscle out of the channel. In this case, the pre-tension is varied easily by pulling the muscle and fixing it in a fixture, which corresponds to a load that provides the same effect. Also, using a longer muscle is more beneficial for observation of the maximum bending angle of the bell segment (25 degrees), since longer muscle has higher displacement which can provide a more accurate reading. The best pre-tensioning for TCP muscle is attained at 800g loading that results in 22.6% actuation strain in air condition at input current of 2.2A for 15s. Further experiments revealed that the length of the muscle does not affect the pre-tensioning results and the same results can be interpreted for all lengths. In **Fig. 5(d)**, the results of the bell actuation with 6-ply TCP at 3 different pre-tensions of 600g (low), 800g (medium), and 1000g (high) are compared underwater. The muscle is actuated for 1.5 s at 8.8A. The high pre-tensioning result in almost 25 degree bending with a higher slope (in a shorter time) in water, however, this pre-tension decreases the lifecycle of the muscle significantly due to the exposure to constant high loading. Due to the stiffness of the 6-ply TCP (calculated as 283 N/m), fixing the actuator at one end and applying the load to the other end, results in specific values of extension of the TCP. The calculated stiffness is comparable to 4-Ply TCP stiffness, which is mentioned as 98.8 N/m by Wu et al.[40]. To pre-tension the muscles, the connected bead wire is pulled through a punched hole on the free end of the spring steel at a calculated length of approximately 1.5cm, and then tied and fixed through the hole. The 1.5 cm is an equivalent of 800g loading for a 95mm actuator before pre-tensioning.

4. Discussion and Conclusion

This paper introduced and described a biomimetic jellyfish (**Fig. 1**) that uses twisted and coiled polymer (TCP) muscle actuators to swim underwater as shown in **Fig. 2(a)**. Similar research efforts were presented that used smart materials as their main source of actuation, however, most utilized some form of metallic SMAs making the presented work novel since we utilized only polymeric materials to produce actuation. The jellyfish robot is created using a 3D printed body, a silicone bell, and TCP actuators making it almost 95% by volume comprised of polymers. The implementation for the TCP actuators in the 3D printed structure rather than the silicone bell serves as a mechanism to maintain the flexibility of the bell, and also the option to easily change, replace, and vary the pre-tension parameters. TCP actuators showed promising results when it is deployed for underwater actuation. Moreover, TCP muscles were preferred over SMA wires due to higher actuation stroke. We have tried to find the optimized working parameters (frequency,

power, and strain) besides some important physical properties of the muscle for actuation such as length and pre-tensioning to generate the best performance of the muscle in the robot. The Poly-Saora jellyfish has the ability to actuate up to eight TCP muscles at once, however, in this case, only four were necessary to swim. The utilization of mainly polymers to create a low-cost actuation mechanism, makes our jellyfish unique and unlike any other conceived. Poly-Saora jellyfish was able to swim 180 mm at speed of 5 mm/s.

The main goal of the current work is utilizing TCP actuators for swimming a biomimetic jellyfish consists of a 3D printed structure and flexible bell segment. Several prototypes are tested for tuning the actuation parameter of TCP with the provided geometry to achieve successful swimming. The robot presented here helped us to test several hypotheses. We did not know which parameter could result in swimming before carrying out experiments. The structure itself, the actuation parameters (amplitude, frequency, and the number of cycles), the number of actuated bell segments, the thickness of the bell, the buoyancy and the pre-stress are some of the important factors for vertical swimming. The main hypothesis in this work is that extremely twisted and coiled polymer (TCP) actuators, when integrated into 3D printed biomimetic structures and flexible substrate, provide a swimming performance if and only if the actuation parameters are tuned with the geometry of the robotic system. We tested several cases and we could not get good performance. The actuation characteristics presented in the summary table (Table 1 and the results in Fig.2) are the ones that resulted good swimming characteristics. These are all associated with the fluid circulation under the bell and the geometry of the bell that caused the fluid flow. The other hypothesis in this work is that the actuation pattern of the flexible bell margin significantly affects the swimming performance, i.e a brief pause during actuation to cool the TCP actuators is essential to allow the flow circulation developed under the bell structure in each swimming cycle.

Future testing and investigation should be focused on creating a fully confined untethered system, that is housed within the 3D printed structure as shown in **Fig. 6**. Environmental sensing components such as temperature sensors, sound sensors, IMU (inertial measurement unit) and a camera can be added to enhance the functionality of the robot for underwater exploration and inspection as shown in **Fig. 6(a)**. Combining these components with a sealed system shown in **Fig 6.(b)** consisting of a communication module, onboard battery, and closed loop control can make the jellyfish swim even more effectively while still maintaining the cost effectiveness offered by the TCP muscles and the polymer passive structures. With the addition of these components and a closed loop control system, we would be taking a big step towards a fully autonomous jellyfish with many applications in exploration and research as shown in **Fig. 6(c)**. A buoyancy control unit and self-contained battery system will also be added to provide autonomy to the robot. **Fig.7, shows the prototypes, which were successfully tested for swimming and we have provided a summary video of the experiments.** We hope these results stand as an important basis for many researchers who would like to investigate the use of these novel TCP actuators for underwater robotic applications.

Acknowledgments

The authors would like to acknowledge the support of the Office of Naval Research (ONR), Young Investigator Program, under Grant No. N00014-15-1-2503. Part of this work is supported by the Office of Naval Research under Contract No. N68335-18-C-0368.

References:

1. Kim, S., C. Laschi, and B. Trimmer, *Soft robotics: a bioinspired evolution in robotics*. Trends in Biotechnology, 2013. **31**(5): p. 23-30.
2. Wang, Z.L., et al., *A micro-robot fish with embedded SMA wire actuated flexible biomimetic fin*. Sensors and Actuators a-Physical, 2008. **144**(2): p. 354-360.

3. Zhou, Y., et al., *A novel biomimetic jellyfish robot based on a Soft and Smart Modular Structure (SMS)*. 2016 Ieee International Conference on Robotics and Biomimetics (Robio), 2016: p. 708-713.
4. Wang, Z.L., et al., *A micro biomimetic manta ray robot fish actuated by SMA*. 2009 Ieee International Conference on Robotics and Biomimetics (Robio 2009), Vols 1-4, 2009: p. 1809-+.
5. Villanueva, A., C. Smith, and S. Priya, *A biomimetic robotic jellyfish (Robojelly) actuated by shape memory alloy composite actuators*. Bioinspiration & Biomimetics, 2011. **6**(3).
6. Shi, L., Shuxiang Guo, and Kinji Asaka, *A Novel Jellyfish-like Biomimetic Microrobot in IEEEIICME International Conference on Complex Medical Engineering 2010*: Gold Coast, Australia
7. Li, T.F., et al., *Fast-moving soft electronic fish*. Science Advances, 2017. **3**(4).
8. Godaba, H., et al., *A Soft Jellyfish Robot Driven by a Dielectric Elastomer Actuator*. Ieee Robotics and Automation Letters, 2016. **1**(2): p. 624-631.
9. Yeom, S.W. and I.K. Oh, *A biomimetic jellyfish robot based on ionic polymer metal composite actuators*. Smart Materials and Structures, 2009. **18**(8).
10. Shi, L., Shuxiang Guo, and Kinji Asaka., *A novel multifunctional underwater microrobot*, in *2010 IEEE International Conference on Robotics and Biomimetics*. 2010: Tianjin, China.
11. Chen, Z., et al., *Bio-Inspired Robotic Cownose Ray Propelled by Electroactive Polymer Pectoral Fin*. Proceedings of the Asme International Mechanical Engineering Congress and Exposition 2011, Vol 2, 2012: p. 817-824.
12. Chen, Z., T.I. Um, and H. Bart-Smith, *Ionic Polymer-Metal Composite Enabled Robotic Manta Ray*. Electroactive Polymer Actuators and Devices (Eapad) 2011, 2011. **7976**.
13. Chen, Z., S. Shatarra, and X.B. Tan, *Modeling of Biomimetic Robotic Fish Propelled by An Ionic Polymer-Metal Composite Caudal Fin*. Ieee-Asme Transactions on Mechatronics, 2010. **15**(3): p. 448-459.
14. Aureli, M., V. Kopman, and M. Porfiri, *Free-Locomotion of Underwater Vehicles Actuated by Ionic Polymer Metal Composites*. Ieee-Asme Transactions on Mechatronics, 2010. **15**(4): p. 603-614.
15. Katzschmann, R.K., et al., *Exploration of underwater life with an acoustically controlled soft robotic fish*. Science Robotics, 2018. **3**(16).
16. Frame, J., et al., *Thrust force characterization of free-swimming soft robotic jellyfish*. Bioinspiration & Biomimetics, 2018. **13**(6).
17. Joshi, A., A. Kulkarni, and Y. Tadesse, *FludoJelly: Experimental Study on Jellyfish-Like Soft Robot Enabled by Soft Pneumatic Composite (SPC)*. Robotics, 2019. **8**(3): p. 56.
18. Najem, J., et al., *Biomimetic jellyfish-inspired underwater vehicle actuated by ionic polymer metal composite actuators*. Smart Materials and Structures, 2012. **21**(9).
19. Haines, C.S., et al., *Artificial Muscles from Fishing Line and Sewing Thread*. Science, 2014. **343**(6173): p. 868-872.
20. Costello, J.H., S.P. Colin, and J.O. Dabiri, *Medusan morphospace: phylogenetic constraints, biomechanical solutions, and ecological consequences*. Invertebrate Biology, 2008. **127**(3): p. 265-290.
21. Tadesse, Y., et al., *Hydrogen-fuel-powered bell segments of biomimetic jellyfish*. Smart Materials and Structures, 2012. **21**(4).
22. Gemmell, B.J., S.P. Colin, and J.H. Costello, *Widespread utilization of passive energy recapture in swimming medusae*. Journal of Experimental Biology, 2018. **221**(1).
23. Gershwin, L.-A., *Jellyfish: A Natural History*. 2016: University of Chicago Press.
24. *Monterey Bay Aquarium Foundation*. 2019 [cited 2019 November 25]; Available from: <https://www.montereybayaquarium.org/animals-and-exhibits/animal-guide/invertebrates/black-sea-nettle>.
25. Saharan, L., et al., *iGrab: hand orthosis powered by twisted and coiled polymer muscles*. Smart Materials and Structures, 2017. **26**(10).

26. Almubarak, Y. and Y. Tadesse, *Twisted and coiled polymer (TCP) muscles embedded in silicone elastomer for use in soft robot*. International Journal of Intelligent Robotics and Applications, 2017. **1**(3): p. 352-368.
27. Haines, C.S., et al., *New twist on artificial muscles*. Proceedings of the National Academy of Sciences, 2016. **113**(42): p. 11709-11716.
28. Haines, C.S., et al., *Artificial muscles from fishing line and sewing thread*. science, 2014. **343**(6173): p. 868-872.
29. Wu, L., et al. *Nylon-muscle-actuated robotic finger*. 2015.
30. Wu, L., I. Chauhan, and Y. Tadesse, *A novel soft actuator for the musculoskeletal system*. Advanced Materials Technologies, 2018. **3**(5): p. 1700359.
31. Gemmell, B.J., Costello, J. H., & Colin, S. P., *Exploring vortex enhancement and manipulation mechanisms in jellyfish that contributes to energetically efficient propulsion*. Communicative & Integrative Biology, 2014. **7**(4): p. e29014.
32. Gemmell, B.J., et al., *Control of vortex rings for manoeuvrability*. Journal of The Royal Society Interface, 2015. **12**(108): p. 20150389.
33. Demont, M.E. and J.M. Gosline, *Mechanics of jet propulsion in the hydromedusan jellyfish, polyorchis pexicillatus: III. A natural resonating bell; the presence and importance of a resonant phenomenon in the locomotor structure*. Journal of Experimental Biology, 1988. **134**(1): p. 347-361.
34. Wu, L. and Y. Tadesse. *Modeling of the Electrical Resistance of TCP Muscle*. in *ASME 2017 International Mechanical Engineering Congress and Exposition*. 2017. American Society of Mechanical Engineers.
35. Wu, L., et al., *Compact and low-cost humanoid hand powered by nylon artificial muscles*. Bioinspiration & biomimetics, 2017. **12**(2): p. 026004.
36. Saharan, L., et al., *iGrab: hand orthosis powered by twisted and coiled polymer muscles*. Smart materials and structures, 2017. **26**(10): p. 105048.
37. Shigley, J.E., *Shigley's mechanical engineering design*. 2011: Tata McGraw-Hill Education.
38. Hughes, T.J., *The finite element method: linear static and dynamic finite element analysis*. 2012: Courier Corporation.
39. Spoon, C. and W. Grant, *Biomechanics of hair cell kinocilia: experimental measurement of kinocilium shaft stiffness and base rotational stiffness with Euler-Bernoulli and Timoshenko beam analysis*. Journal of Experimental Biology, 2011. **214**(5): p. 862-870.
40. Wu, L., et al. *A reconfigurable robot with tensegrity structure using nylon artificial muscle*. in *Active and Passive Smart Structures and Integrated Systems 2016*. 2016. International Society for Optics and Photonics.
41. Villanueva, A., et al., *Jellyfish inspired unmanned underwater vehicle*. SPIE Smart Structures and Materials + Nondestructive Evaluation and Health Monitoring. Vol. 7287. 2009: SPIE.
42. Cheng, T.Y., et al., *Untethered soft robotic jellyfish*. Smart Materials and Structures, 2019. **28**(1).
43. Kazemi-Lari, M.A., et al. *Robotic jellyfish actuated with a shape memory alloy spring*. in *Bioinspiration, Biomimetics, and Bioreplication IX*. 2019. International Society for Optics and Photonics.
44. Ko, Y., et al., *A jellyfish-like swimming mini-robot actuated by an electromagnetic actuation system*. Smart Materials and Structures, 2012. **21**(5).
45. Nawroth, J.C., et al., *A tissue-engineered jellyfish with biomimetic propulsion*. Nature Biotechnology, 2012. **30**(8): p. 792-797.
46. Marut, K., et al., *A jellyfish-inspired jet propulsion robot actuated by an iris mechanism*. Smart Materials and Structures, 2013. **22**(9).

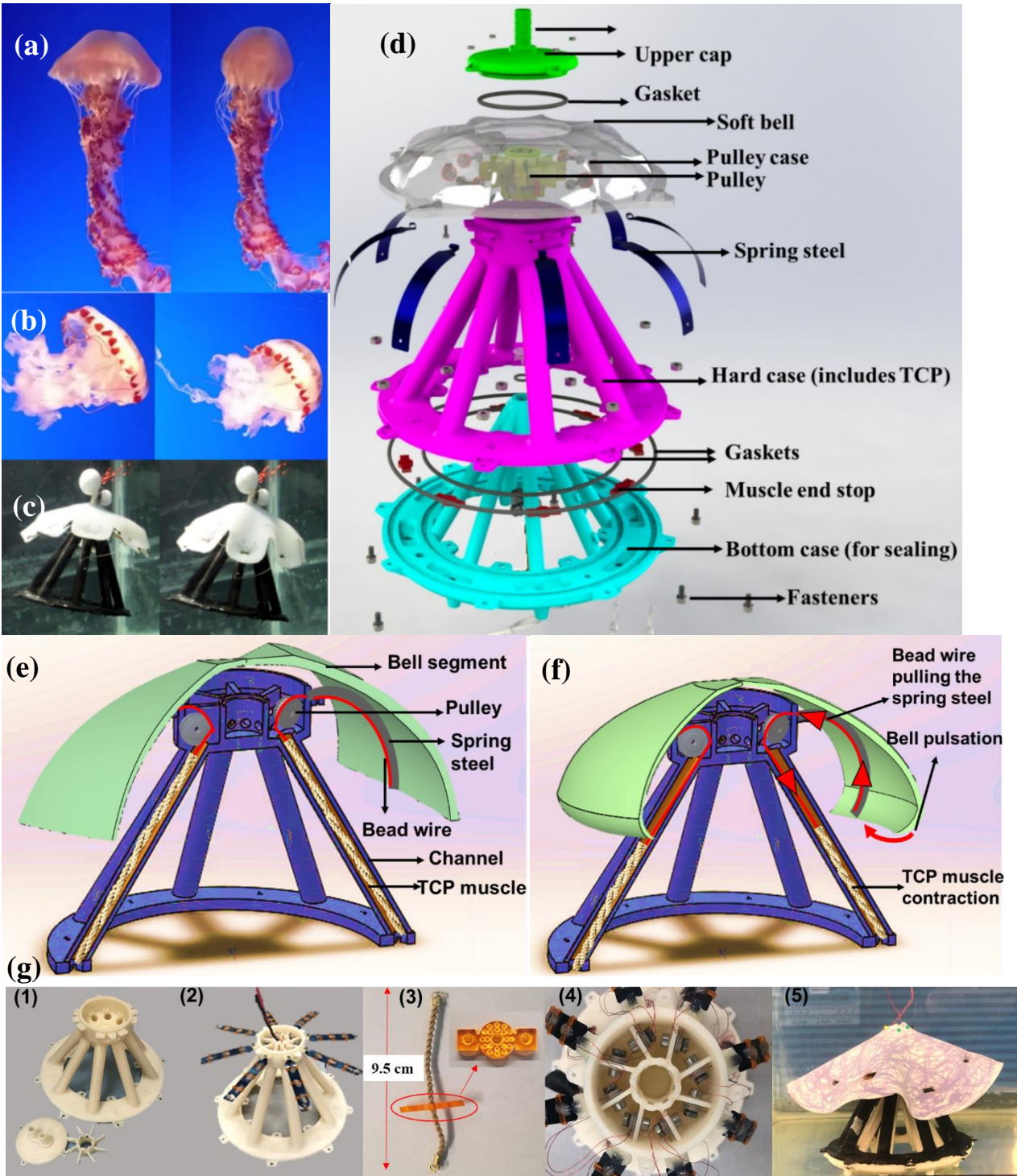


Figure 1. Biomimetic jellyfish robot with polymer muscles inspired by biological models (a) Black sea nettle (*Chrysaora Achlyos*), (b) Purple striped jellyfish (*Chrysaora Colorata*); (c) bio-inspired vehicles (bottom) used TCP muscles to float gracefully underwater. (d) Exploded view of jellyfish robot structure design with all components. (e) The parts involved in bell actuation mechanism at the relaxed configuration, (f) bell actuation mechanism at contraction state, (g) manufacturing process of the jellyfish structure: (1) 3D printed plastic parts for hard case, (2) Prepare the structure by first attaching the spring steels, (3) TCP muscle prepared for inserting in the channel along with end stop, (4) the pulley casing for transmitting the linear contraction of the muscle to actuate the bell, (5) the final jellyfish structure.

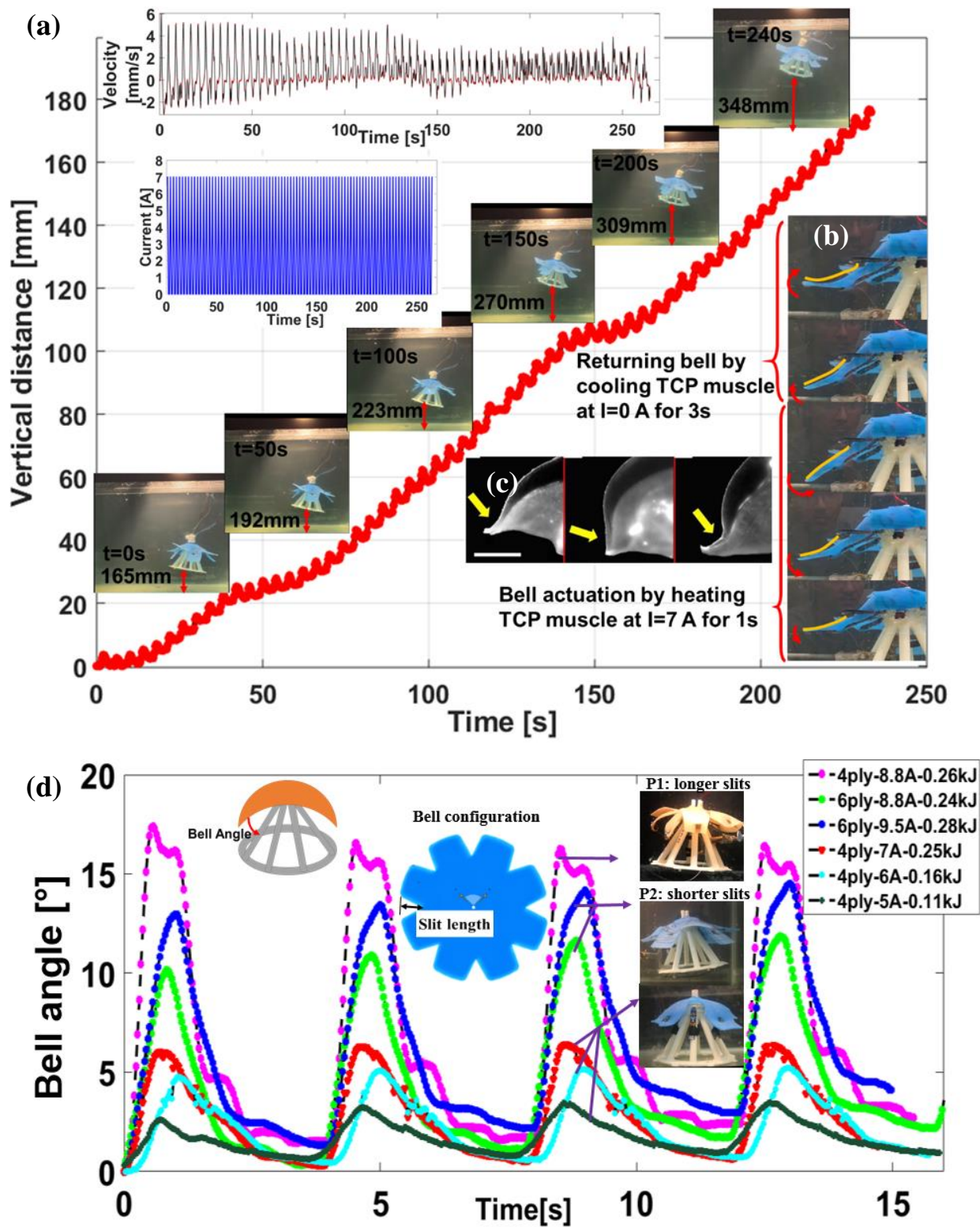
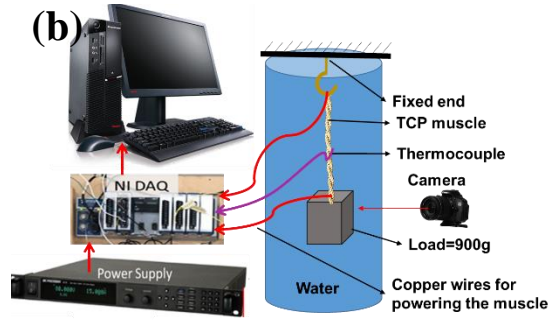
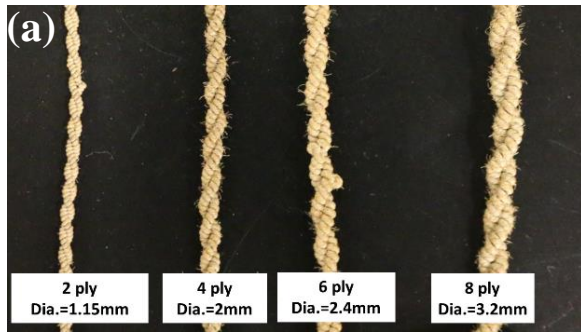
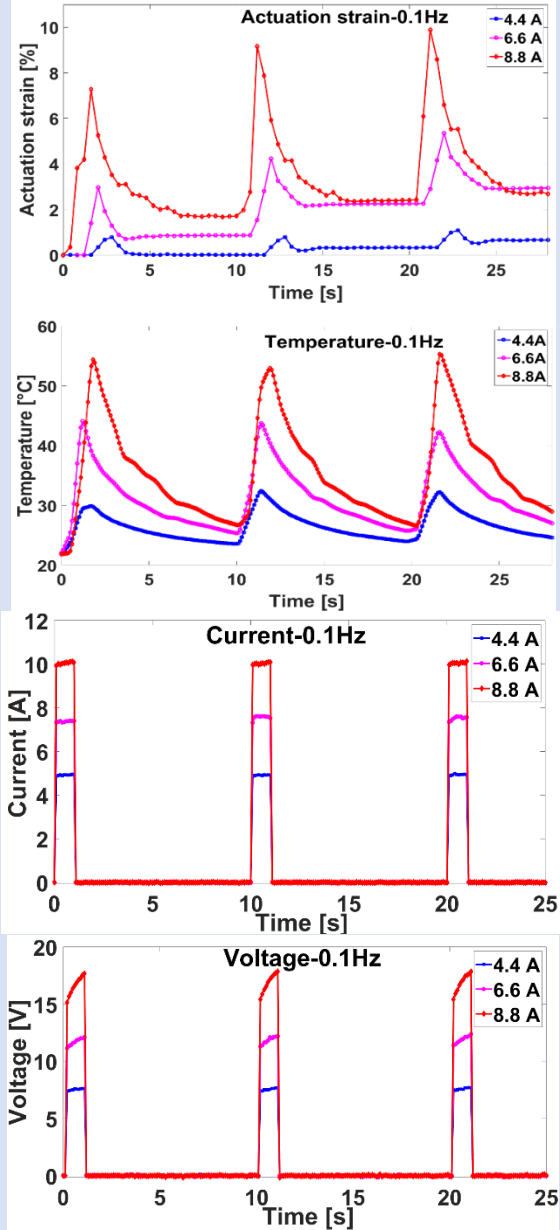


Figure 2. Biomimetic jellyfish swimming test with 6ply TCP: (a) vertical position, velocity, input current, and bell deformation during actuation and cooling; (b) bell deformation of jellyfish robot during swimming compared to (c) deformation of bell margin during swimming in real jellyfish species (*Aurelia aurita*) [19]. (d) Result of the actuation of one bell segment underwater with 4ply and 6ply TCP muscles (length $L = 95$ mm, 800g pre-tension) at different input powers.



(c) $f=0.1$ Hz



(d) $f=0.25$ Hz

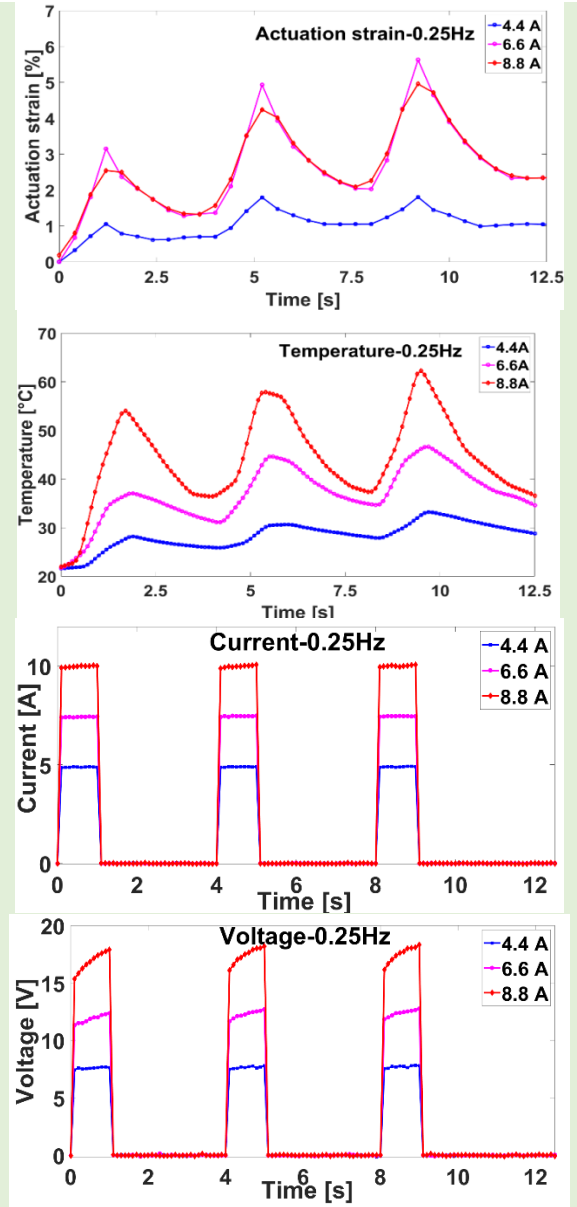


Figure 3. Characteristics of TCP muscles : (a) multi-ply TCP muscles, (b) underwater characterization experimental set up, characteristics of 6ply TCP muscle in water carrying 900g load and actuated at an input current of 4.4A, 6.6A and 8.8A (c) at frequency =0.1 Hz (1s heating and 9s cooling) and (d) at frequency= 0.25Hz (1s heating and 3s cooling).

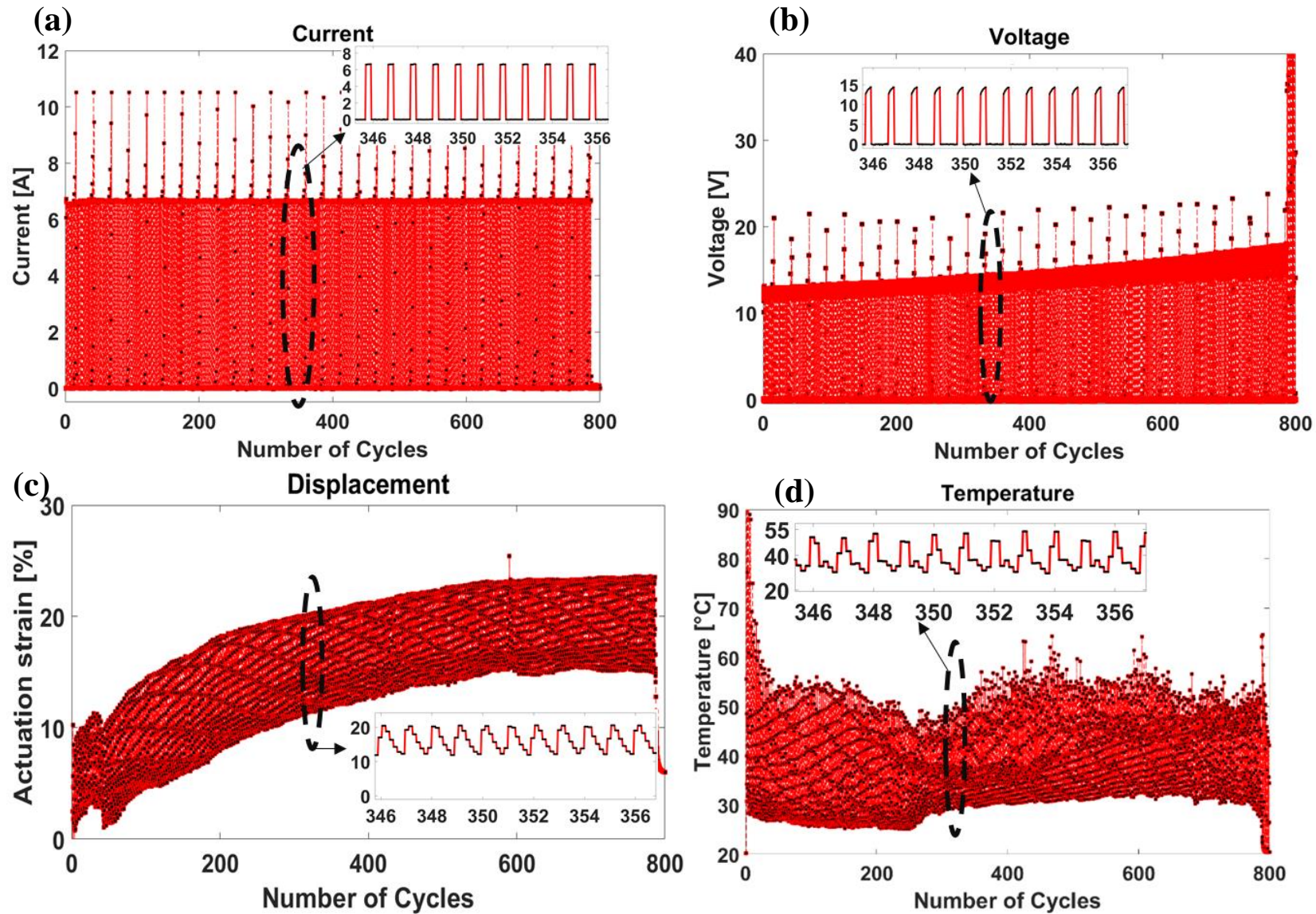


Figure 4. Life cycle test of 6ply TCP at 6.5A current and frequency of 0.25 Hz (1 s heating and 3 s cooling): (a) input current ;(b) output voltage, (c) actuation strain (output) and (d) actuation temperature.

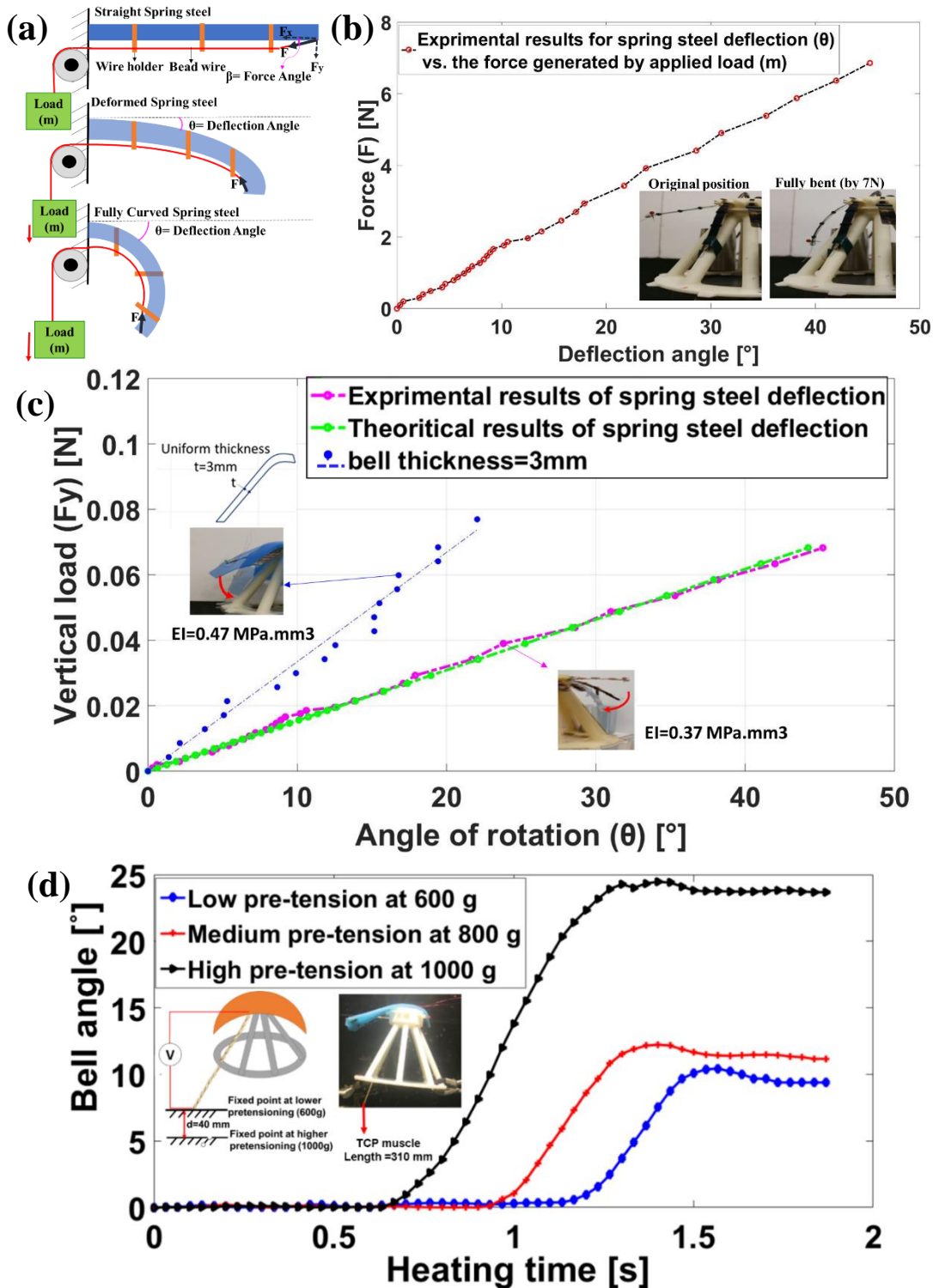


Figure 5. Bell deformation mechanism and analysis, and the effect of pre-tensioning the TCP on bell deformation in water: (a) Schematic of bell deformation mechanism, (b) relation between the deformation angle (θ) and the applied force (m), (c) the angular displacement of the bell with and without soft compartment vs vertical load (F_y), and (d) the results of actuation of the TCP at low (600g), medium (800g) and high (1000g) pre-tensioning. The pre-tensioning is changed by the fixed end of a long muscle ($L=310 \text{ mm}$) outside the channel tube as shown in the plot asset.

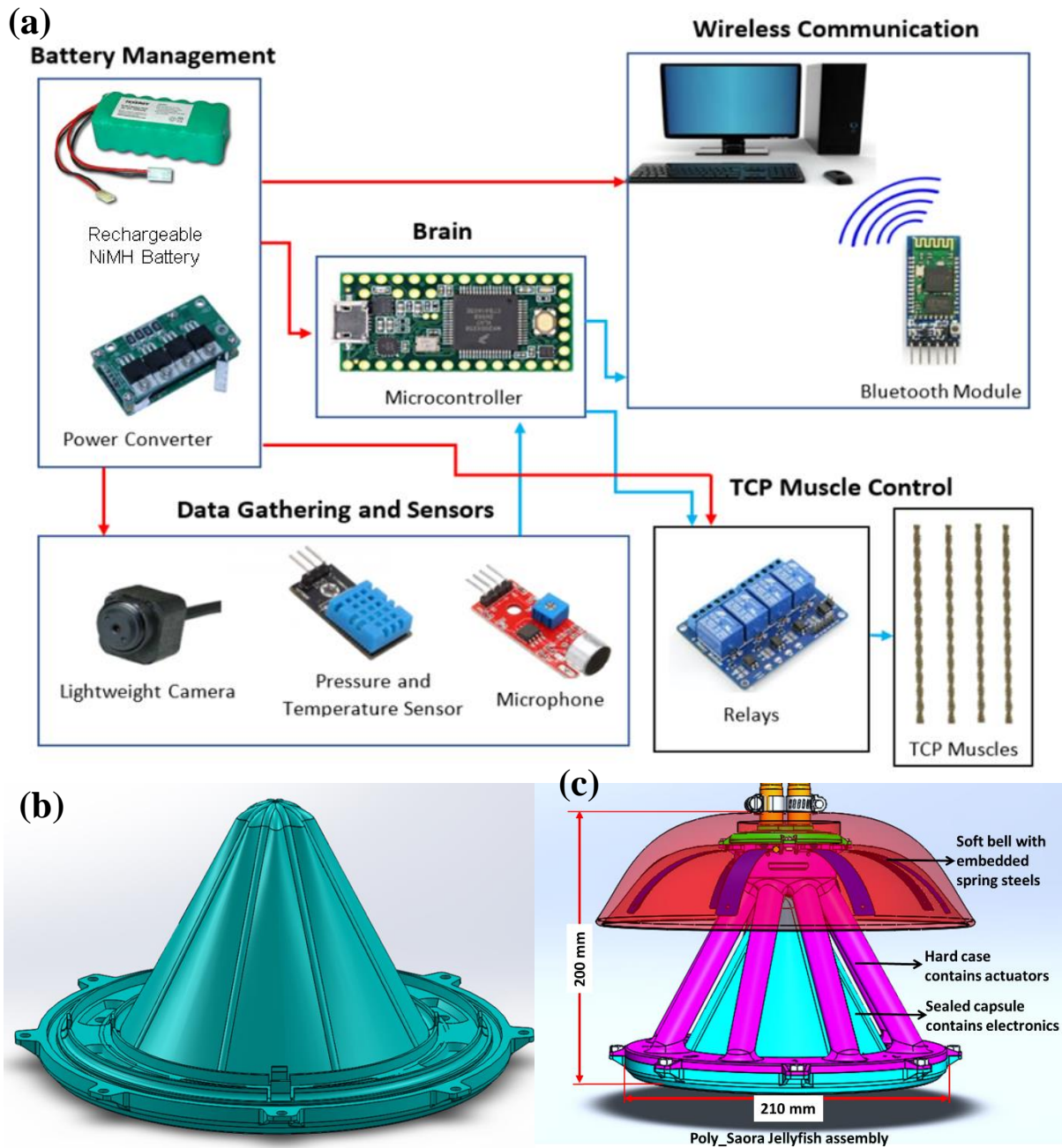


Figure 6. (a)Proposed design circuit for untethering powering and control of Poly-Saora, (b) designed capsule for accommodating electronic components and (c) assembly of the powering and control unit under the robot.

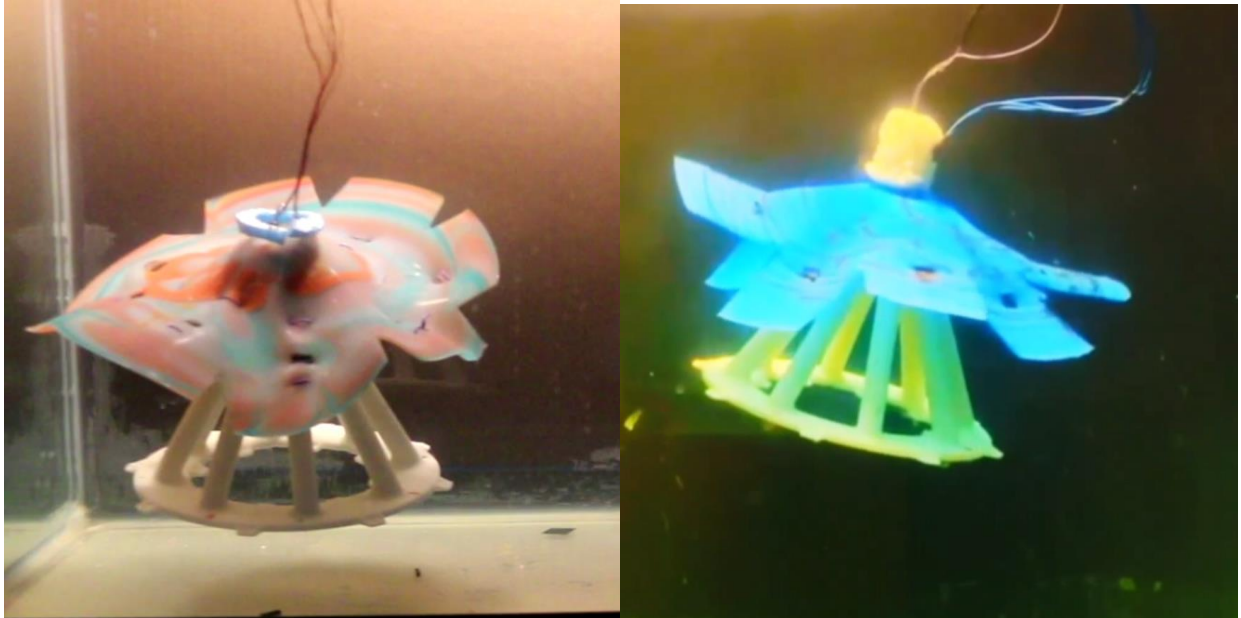


Figure 7. Jellyfish prototypes which successfully swim in the water by implementing 6-ply TCP muscle for actuation.

Table 1. Comparison of swimming jellyfish robots.

	Reference	Size	Actuator	Swimming Speed (mm/s)	Power Consumption			Actuation Frequency (Hz)
					Voltage (V)	Current (A)	Power (W)	
Non-conventional actuators	Yeom, S.W, and Il-Kwon Oh. [9], 2009	30mm dia.	IPMC	0.057 (max)	3	-	-	1
	Villanueva, Y., et al.[41], 2009	450cm ³ (324g)	SMA	78	-	3.5	19.2	1
	Villanueva, A., et al.[5], 2011.	164mm dia. (200 cm ³ , 242g)	SMA	54.2	-	1.5	~ 120 (peak)	0.5
	Najem J, et al. [18], 2012	150mmx58mm dia.,20g	IPMC	0.77 (4 bells)	2	-	0.7	0.1 – 10
				1.5 (8 bells)	2	-	1.14	
	Godaba H, et al.[8], 2016	140mmx118mm (500g)	Dielectric elastomer	10	6000	-	-	-
	Zhou, Y., et al.[3], 2016	216mmx68mm dia.,20g	SMA	111	-	1	-	1
	Cheng, T., et al.[42], 2019	150mmx90mm(28g)	Dielectric Elastomer	10 (Tethered)	7000	-	-	1.9
				5 (Untethered)	9000	-	-	1.6
	Kazemi-Lari, M. A., et al.[43], 2019	76mm (40.1g)	SMA coils	6	18-19	-	104-115	0.5
Hamidi, A, et al. (Poly Saora), 2019	220mm (diameter) x 200 mm (height) (440g)	Nylon 6,6 TCP_{Ag}	5	20	30	600	0.25	
Conventional/Other	Ko, Y., et al.[44], 2012	17mm, 0.14g	Magnetic	-	-	13	-	10
	Nawroth J C et al. [45], 2012	10mm dia.	Bioengineered tissue	10	-	-	-	-
	Marut, K., et al. [46], 2013	5.7cmx7.9cm (46.5cm ³ ,80g)	iris mechanisms	116	10	-	-	-
	Frame J, et al.[16], 2018	210mm dia. (380g)	Hydraulic	30	-	-	2.29 – 5.58	0.435 – 0.8
	Joshi et al. [17], 2019	220 mm dia. (500g)	Pneumatic	160	12	-	-	0.8

Table 2. Properties of the 6ply Ag-TCP used in one bell of Poly-Chrysa jellyfish while swimming

Parameter	Value	
Material	Silver coated nylon 6,6	
Mass (measured using high precision scale)	$m = 0.841\text{g}$	
Type of actuation	Electrothermal	
diameter	$D_1 = 2.4\text{ mm}$	
Length of precursor fiber	$L = 95\text{ mm}$	
Specific heat capacity	$C_p = 1700\text{ J/Kg}^\circ\text{C}$	
Resistance	$R_1 = 2.5\ \Omega$	
Pretension (grams)	$W = 900\text{g}$	
Actuation environment	Air	Water
Current	$I_a = 2.2\text{ A}$	$I_w = 7.5\text{ A}$
Voltage	$V_a = 5.5\text{ V}$	$V_w = 20\text{ V}$
Heating time	$t_h = 15\text{ s}$	$t_h = 1\text{ s}$
Cooling time	$t_c = 45\text{ s}$	$t_c = 3\text{ s}$
Heating energy	$E_h = 181.5\text{ J}^{**}$	$E_h = 160\text{ J}^*$
Actuation frequency (While swimming)	$f = 0.25\text{ Hz}$	$f = 0.25\text{ Hz}$
Lifecycle of TCP	$\eta = 200\text{ cycles [25]}$	$\eta = 787\text{ cycles}$
*The actuation strain at 160J heating energy in air condition is ~8%.		
** The actuation strain at 181.5J energy in water condition is ~22%.		